In Situ Photopolymerization Behavior of Chiral Liquid-Crystalline Monomers and Image Storage Using Ferroelectric Properties

Sayuri Ogiri, Hiroyuki Nakamura, Akihiko Kanazawa, Takeshi Shiono, and Tomiki Ikeda*

Research Laboratory of Resources Utilization, Tokyo Institute of Technology, 4259 Nagatsuta, Midori-ku, Yokohama 226-8503, Japan

Isa Nishiyama

Japan Energy Corporation, Ltd., 3-17-35 Niizo-Minami, Toda, Saitama 335, Japan

Received April 10, 1998; Revised Manuscript Received March 28, 1999

ABSTRACT: We report in situ photopolymerization behavior of ferroelectric liquid-crystalline (FLC) monomers with the polymerizable group attached to the rigid core through a long methylene spacer (carbon number of 11, **MS11**) and a short methylene spacer (carbon number of 2, **MS2**) and image storage using bistable switching of FLC monomers by applying an electric field. The polymerization behavior of **MS2** was considerably different from that of **MS11**. This might be due to a higher concentration of the polymerizable groups in **MS2**. In addition, the relative conversion (the ratio of conversion under electric field to that without electric field) in the SmC* phase of **MS2** was larger than that of **MS11**. This result suggests that the change in macroscopic structure is more effective in the polymerization of **MS2** in which the polymerizable groups are more densely packed. Furthermore, the image storage was performed by in situ photopolymerization with a dc electric field.

I. Introduction

The chiral smectic C (SmC*) phase of ferroelectric liquid crystals (FLCs) exhibits spontaneous polarization (Ps) because of the presence of polar groups which give the molecules an electric dipole moment. In the SmC* phase, the FLC molecules are aligned parallel to each other to form a layer with a tilt between the direction of the long axis of the FLC molecule and the normal to the smectic layer.[1,2] The average direction of the molecular long axis is defined as the director in each layer, and owing to the chiral group in the FLC molecules, the director adopts a helicoidal structure with a characteristic pitch. When the FLC molecules are placed in a cell with a small gap (<2 μm), which is smaller than the helical pitch, the interaction of the FLC molecules and the cell surface is so strong that the helix structure becomes energetically unfavorable, and the director in every layer is aligned in the same direction with the smectic layers oriented roughly perpendicular to the cell surface. As a result, the polarization of all layers is also aligned in one direction.[2] If an external electric field is applied across the cell, the polarization can be aligned upward or downward, depending on the polarity of the applied electric field. When the polarity of the electric field is reversed, the polarization flips. These two stable states are called surface-stabilized states, and FLCs exhibit bistability.[1a]

Highly oriented polymers exhibit anisotropy of optical, electrical, and thermomechanical properties. Polymerization of LC monomers has been conducted extensively to obtain polymer liquid crystals (PLCs).[3] The LC monomers can be macroscopically oriented by external forces, such as an electric or a magnetic field, elongational flow, and surface orientation. Monomer organization may affect the polymerization kinetics, the polymer structure, and the microstructure of polymers.[4] If polymerizable FLCs are used, it is assumed that the polymerizable groups adjoin and are aligned in one direction in each layer of the SmC* phase. In situ photopolymerization of FLC monomers, which offers an advantage in that the temperature can be chosen precisely, is expected to show specific polymerization behavior. The effect of LC ordering on the rate of free-radical polymerization of mesomorphic vinyl monomers has been discussed extensively.[3,5] If an alkyl spacer between the polymerizable group and the rigid core is long, the orientation of the polymerizable groups is disordered even though the core part of the mesogens is highly oriented. With a short spacer, the orientation of mesogens affects that of polymerizable groups, improving molecular packing in an LC phase.[6]

In the previous paper, we reported in situ photopolymerization behavior of FLC monomer possessing a long spacer.[7] However, photopolymerization behavior of FLC monomers which have a short spacer has not yet been reported. In this study, we synthesized chiral LC vinyl monomers with methacrylate group attached to the rigid core through a short methylene spacer (carbon number of 2) and a long methylene spacer (carbon number of 11) and investigated the LC behavior of these monomers. We next explored the effect of molecular packing of the LC monomers on polymerization behavior by photoinitiation which can be done at any temperature after complete equilibrium of LC ordering of the LC monomers is attained. Furthermore, image storage was examined by means of in situ photopolymerization under a dc electric field.

II. Experimental Section

II.1. Materials. II.1.1. FLC Monomers. The structures of the two FLC monomers, [*R*]-1-methylheptyl 4′-[4-(*ω*-methacryloyloxyundecyloxy)benzoyloxy]biphenyl-4-carboxylate (**MS11**), [*R*]-1-methylheptyl 4′-[4-(*ω*-methacryloyloxyethoxy)benzoyloxy]-

* To whom correspondence should be addressed.

10.1021/ma9805607 CCC: $18.00
Published on Web 07/02/1999

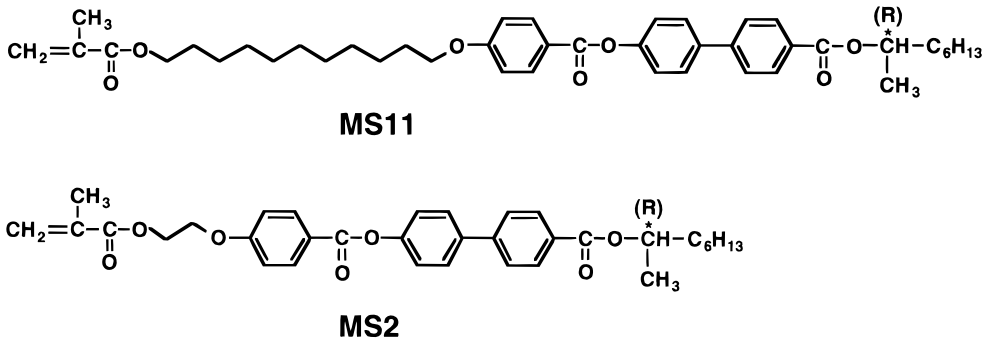

Figure 1. Chemical structures of the FLC monomers used in this study.

biphenyl-4-carboxylate (**MS2**), used in this study are shown in Figure 1. The FLC monomers were prepared according to the synthetic method reported previously.[8] The compounds were characterized by means of ^{1}H NMR (Bruker AC200, 200 MHz), IR (Hitachi 260-10), and elemental analysis. The phase transition temperature and the phase structure were determined by differential scanning calorimetry (DSC; Seiko I&E SSC-5200 and DSC220C; cooling rate, 1 °C/min) and optical polarizing microscopy (Olympus Model BH-2; Mettler FP82HT hot stage and Mettler FP90 central processor).

II.1.2. Preparation of Phase Diagram. Before evaluation of the in situ photopolymerization behavior of the monomeric FLCs, we investigated the phase transition behavior during polymerization, since it was found that, during photoirradiation, the phase transition temperature changed with the change in composition of the monomer−polymer mixture. To prepare the phase diagram in the binary mixture of the polymer and the monomer, the FLC polymers were synthesized by the conventional solution polymerization.[7] The number-average molecular weight (M_n) and polydispersity (M_w/M_n) was determined by gel permeation chromatography (GPC, JASCO GULLIVER SERIES; column, Shodex GPC K802 + K803 + K804 + K805; eluent, chloroform) calibrated with standard polystyrenes using UV−vis detector (λ = 254 nm). The phase transition temperature and the phase structure were identified by DSC (10 °C/min) and optical polarizing microscopy.

II.2. In Situ Photopolymerization Procedure. Photopolymerization was performed in a glass cell with a gap of 2 μm without an electric field or under a dc electric field of 3 V/μm. The glass cell was composed of two indium tin oxide (ITO) glass substrates with polyimide alignment layers rubbed in an antiparallel direction. Samples for photopolymerization were prepared by injecting the FLC monomer containing 1-hydroxycyclohexyl phenyl ketone as a photoinitiator (2 mol %) into the glass cell in the I phase at 85 °C using capillary action. It was confirmed that the concentration of the photoinitiator was too small to destabilize the LC phases, and no spontaneous thermal polymerization occurred during injection of the FLC monomers into the glass cell. Furthermore, it was confirmed that, without the photoinitiator, the photopolymerization could not be initiated even after prolonged photoirradiation at 366 nm. After the samples were prepared, they were cooled slowly (0.5 °C/min) to a polymerization temperature. Photoirradiation was performed with a 500 W high-pressure mercury lamp, and the 366-nm line (intensity, 1 mW/cm^2 or 0.1 mW/cm^2) was isolated by a combination of glass filters (Toshiba; UV-D36C, UV-35, IRA-25S). The light intensity was measured with a power meter (TQ 8219). In the photopolymerization under an electric field, the samples were cooled slowly under ac electric field (1 Hz, ± 3 V_{pp}/μm) to the temperature for photopolymerization. After a ferroelectric monodomain structure was obtained at the temperatures for which the ferroelectric electrooptic response in the SmC* phase was fully developed, the cell was irradiated at 366 nm with the dc electric field of 3 V/μm during polymerization.

The course of the polymerization was followed by GPC. The conversion was estimated from eq 1, where P is the peak area

$$\text{conversion (\%)} = P/(P + M) \times 100 \qquad (1)$$

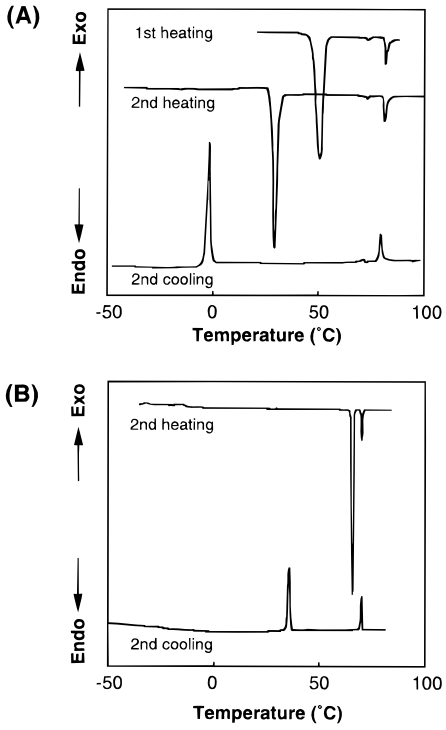

Figure 2. DSC thermograms of FLC monomers at heating and cooling rate of 1 °C/min: (A) **MS11**; (B) **MS2**.

in the GPC chart corresponding to the polymers produced and M is that corresponding to the unchanged monomers. Each GPC measurement was repeated, and we confirmed that the reproducibility of the conversion and the molecular weight was invariably good.[7]

III. Results and Discussion

III.1. Phase Transition Behavior of FLC Monomers and Polymers. Before the polymerization behavior was explored, the phase transition behavior of monomers was investigated. Figure 2 shows the DSC thermograms of the FLC monomers. The FLC monomers exhibited several sharp endothermic (heating) and exothermic (cooling) peaks. Referring to the optical microscopic observation, the phases could be assigned to crystalline (K), antiferroelectric chiral smectic C (SmC_A*), SmC*, chiral smectic A (SmA*), and isotropic (I) phases. The temperature and enthalpy for each phase transition are summarized in Table 1. Table 2 lists the M_n, M_w/M_n and phase transition temperature of each polymer obtained by solution polymerization.

III.2. In Situ Photopolymerization Behavior. It is important to evaluate the changes in the phase transition temperature due to changes in composition

Table 1. Phase Transition Temperature[a] and Change in Enthalpy[b] of Transition of FLC Monomers

compd		phase transition temp (°C)
MS11	first heating	K 50 (45); SmC* 73 (0.55); SmA* 81 (3.4); I
	second heating	K 29 (48); SmC* 73 (0.48); SmA* 81 (4.3); I
	second cooling	I 80 (3.7); SmA* 72 (0.55); SmC* 55 (*c*); SmC_A* −1.7 (21); K
MS2	second heating	K 66 (29); SmA* 70 (3.5); I
	second cooling	I 70 (3.0); SmA* 47 (0.50); SmC* 35 (13); K

[a] Key: K, crystal; SmC_A*, antiferroelectric chiral smectic C; SmC*, ferroelectric chiral smectic C; SmA*, chiral smectic A; I, isotropic. [b] The values in parentheses give the change in enthalpy of transition in kJ/mol. [c] The change in enthalpy of the SmC*−SmC_A* transition was too small to be evaluated.

Table 2. M_n, M_w/M_n and Phase Transition Temperature[a] of the Polymer by Solution Polymerization

compd	M_n	M_w/M_n	phase transition temp (°C)
poly(MS11)	6.4×10^4	3.5	G 37; SmC_A* 150; SmA* 161; I
poly(MS2)	6.3×10^4	4.1	G 138; SmA* 220; decomp

[a] Key: G, glassy; SmC_A*, antiferroelectric chiral smectic C; SmA*, chiral smectic A; I, isotropic.

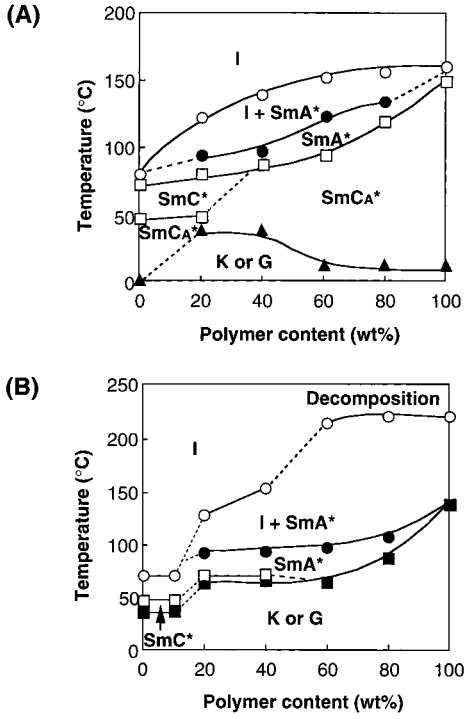

Figure 3. Phase diagrams for mixtures of monomer and polymer: (A) **MS11**; (B) **MS2**.

of the monomer−polymer mixture.[9] Several samples were prepared in which the mixing ratio of the monomer and the polymer was altered, and the binary mixtures were subjected to DSC and microscopic observation to explore the phase behavior. The phase diagram is shown in Figure 3. In both systems, phase transition occurred as the ratio of the monomer to polymer changed. In the case of **MS11** with a relatively low polymer content (less than 20 wt %), the phase transition temperature changed only slightly. This result demonstrates that the change in the phase structure could be negligible in the early stage of polymerization. The phase transition temperature of the mixtures was, however, shifted to higher temperature as the polymer content increased, and the temperature range of the SmC_A* phase increased considerably. For **MS2** at a relatively low polymer content, the phase transition temperature changed, but to a lesser extent. On the other hand, the phase structure changed considerably as the polymer content increased.

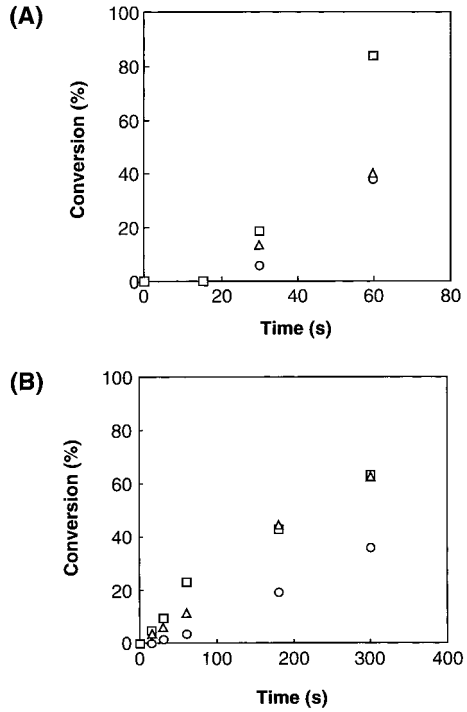

Figure 4. Time−conversion curves for photopolymerization at various temperatures in glass cell with a gap of 2 μm: (A) on photoirradiation (1 mW/cm^2) of **MS11**; (B) on photoirradiation (0.1 mW/cm^2) of **MS2**. Key: (○) 40 °C; (□) 60 °C; (△) 80 °C.

The time−conversion curve obtained by photoirradiation of **MS11** at a light intensity of 1 mW/cm^2 is shown in Figure 4A and that of **MS2** at 0.1 mW/cm^2 in Figure 4B. The conversion showed a tendency to increase with increasing irradiation time, irrespective of the polymerization temperature. A similar trend was observed for samples under an electric field. However, time−conversion profiles were observed to be considerably different due to the condition of the applied electric field. On the basis of the phase diagram shown in Figure 3, it is assumed that no phase transition occurs at least on 30-s irradiation of **MS11** due to the low content of the polymer produced. We therefore used the conversions after 30-s irradiation as a measure to explore the in situ photopolymerization behavior of the **MS11** monomer. On the other hand, for **MS2**, the conversions after photoirradiation at 1 mW/cm^2 were high and it was assumed that phase transition occurred during polymerization. At 0.1 mW/cm^2, conversions after 60-s irradiation were relatively low, and no phase transition was expected during polymerization.

III.2.1. Polymerization Behavior of MS11 Monomer. Figure 5A shows GPC charts of samples after photopolymerization of **MS11** in the SmC* phase at 60 °C. At low conversion (19% conversion), a monomodal peak of polymer was observed, although at high conver-

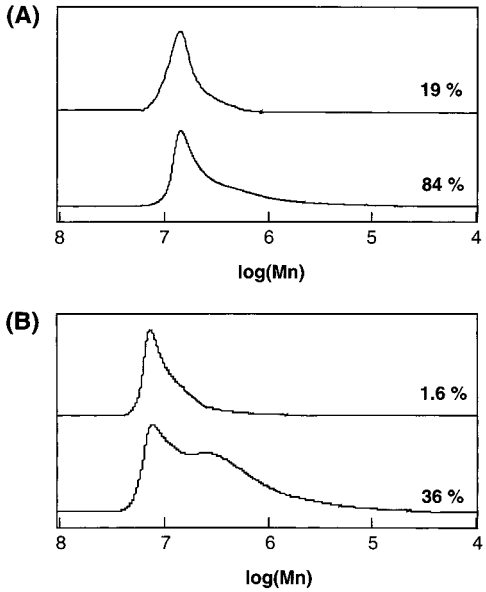

Figure 5. GPC charts of samples after photopolymerization of FLC monomers in glass cell with a gap of 2 μm: (A) after irradiation (1 mW/cm^2) of **MS11** at 60 °C; (B) after irradiation (0.1 mW/cm^2) of **MS2** at 40 °C. Numbers in the figure show conversion.

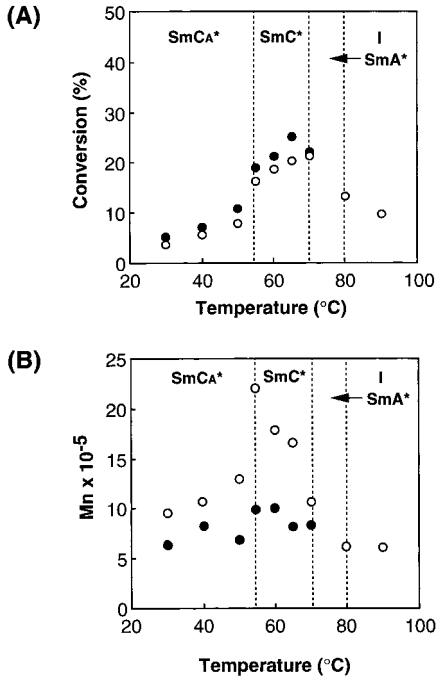

Figure 6. Polymerization behavior of **MS11** after 30-s photoirradiation (1 mW/cm^2) at various temperatures in a glass cell: (A) conversion; (B) number-average molecular weight. Key: (○) without an electric field; (●) with a dc electric field of 3 V/μm.

sion (84% conversion) the peak showed a shoulder. It has been reported that the phase transition to the Sm phase occurred during polymerization of monomer with the cholesteryl group in the cholesteric (Ch) phase, and a peak in the higher molecular weight fractions appeared in the GPC chart.[10] The formation of a polymer with a lower molecular weight may be related to the extremely small rate constant of propagation due to the high viscosity of the system. It can therefore be presumed that the polymerization behavior changed at high conversion because of a phase transition to the viscous SmC_A* phase during polymerization.

The relation between conversion and temperature in photopolymerization of **MS11** is shown in Figure 6. Conversions after 30-s irradiation were plotted as a function of temperature. Without the electric field, conversion was highest in the SmC* phase (Figure 6A,○). The distances between polymerizable groups become small when the monomer shows a high orientation. From the standpoint of the kinetics, it may be assumed that in the SmC* phase the rate constant of propagation (k_p) is small, while that of termination (k_t) is much smaller because of high viscosity with low mobility. Therefore, it is anticipated that conversion is high. The conversion of the corresponding acrylate in the SmC* phase was as high as that in the SmC_A* phase in the early stage of polymerization,[7] while the polymerizability of **MS11** in the SmC_A* phase descreased. The conversions of **MS11** after 15-s irradiation were 0% irrespective of polymerization temperature, whereas those of the acrylate were 10% even after 5-s irradiation in the SmC* phase. In general, k_p increases with polymerization temperature, and k_p's for acrylates are approximately 5 (30 °C) and 2.5 (50 °C) times as large as those for methacrylates.[11] Consequently, it is expected that kinetic factors such as k_p are responsible for the difference in polymerizability between methacrylate and acrylate, and this difference is larger at lower temperatures. In addition, conversion decreased in the I phase. These results indicate that the k_p in organized system is dependent on molecular alignment as well as mobility. On the other hand, M_n was largest at the SmC_A*−SmC* phase transition temperature (Figure 6B,○). This result differs from those of the acrylate.[7] Since resonance effect is higher for methacrylate radicals, the lifetime of the methacrylate radicals may be longer than that of acrylates. The difference in reactivity and lifetime of propagating radicals seems to result in the observed difference in polymerization behavior between the methacrylate and the acrylate. In contrast, M_n of the resultant polymethacrylate was almost the same as that of the polyacrylate. Kinetic chain length related to M_n is proportional to the ratio of k_p to k_t in the steady state, and hence the similarity in M_n implies that the ratios of these two rate constants may be similar between the methacrylate and the acrylate.

III.2.2. Polymerization Behavior of MS2 Monomer. MS2 having a short spacer exhibited a polymerization behavior different from that of **MS11**. At a light intensity of 0.1 mW/cm^2, the formation of polymer was confirmed in **MS2** but not in **MS11** by GPC. It is obvious that functional groups are densely located in the case of **MS2** because the number of polymerizable groups in unit volume is larger in **MS2** than in **MS11**. It is reasonable to assume that polymerizability depends on the density of the polymerizable groups. At 1 mW/cm^2, conversion and M_n were independent of the initial phase of monomer and applied electric field in the polymerization of **MS2**. This implies that the phase transition to K or G phase occurred during polymerization as demonstrated in Figure 3. To investigate the effect of phase structure of monomer on polymerization behavior, photopolymerization was conducted at a lower light intensity of 0.1 mW/cm^2. When the light intensity was low, a phase transition did not occur during polymerization due to low conversion.

Figure 5B shows charts of samples after photopolymerization of **MS2** in the SmC* phase at 40 °C. Even at

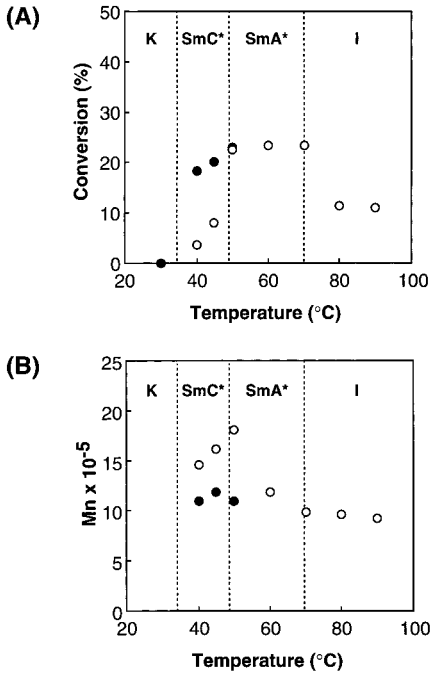

Figure 7. Polymerization behavior of **MS2** after 60-s photoirradiation (0.1 mW/cm^2) at various temperatures in a glass cell: (A) conversion; (B) number-average molecular weight. Key: (○) without an electric field; (●) with an electric field of 3 V/μm.

low conversion (1.6% conversion), a shoulder in the peak was observed. The M_n of the higher molecular weight part was approximately twice as large as that of the lower molecular weight part. For **MS11**, a monomodal peak was observed in the early stage of polymerization. It can therefore be assumed that two active species exist in the polymerization mixture of **MS2** with different microenvironments even though no change in the macroscopic phase structure was observed. At high conversion (36% conversion), a large portion of the low molecular weight fraction was observed in the GPC charts. Transition of the polymerization mixture to the G phase at high conversion might significantly have retarded the polymerization.

Figure 7 shows conversion (A) and M_n (B) in the polymerization of **MS2** as a function of temperature. Conversion was low in the SmC* phase without electric field, whereas conversion in the SmC* phase with a dc electric field was as high as that in the SmA* phase. The SmC* phase with a dc electric field shows extremely high orientation and the polymerizable groups may be closely located, which results in high conversion. M_n increased with temperature in the SmC* phase without electric field. This is due to the decrease of the low molecular weight fraction in the GPC chart at high temperature in the SmC* phase. M_n was largest at the SmC*−SmA* phase transition temperature and decreased as the temperature increased in the SmA* phase. In the early stage of polymerization in the SmA* or I phase, the peak in the GPC chart was monomodal and M_n was lower than that in the SmC* phase. The decrease in M_n of polymer obtained in the SmA* phase may be ascribed to the occurrence of a chain transfer reaction.

III.2.3. Effect of Electric Field on Polymerization. It is expected that the polymerization rate would be enhanced significantly when the FLC monomers are highly aligned by application of the electric field. Such effects of the external electric field on the polymerization rate have been observed also for a chiral LC monomer showing the SmA* phase, and the polymerization rate seems to be dependent on the efficient collision between polymerizable groups.[12] However, it has been also reported that the change of the macroscopic alignment by external forces does not alter the polymerization kinetics.[3j] The result obtained in this study shows that conversion increased and M_n of the polymer produced decreased under a dc electric field compared to those without electric field (Figures 6 and 7). To compare polymerization behavior between two monomers which have different lengths of the alkyl spacer, we evaluated the relative conversion (the ratio of conversion under electric field to that without electric field) in the SmC* phase. It was found that the relative conversion of **MS2** was 3.1 and that of **MS11** was 1.2. As described in the previous section, if the spacer is long, the orientation of polymerizable groups of LC monomers is poor even though the core is highly oriented, whereas the orientation of mesogens affects that of functional groups for monomer possessing a short spacer. Thus, the change of macroscopic structure was more effective in the polymerization of **MS2** having a short spacer.

The monomer shows high orientation (ferroelectric surface-stabilized state) by applying a dc electric field in the SmC* phase where the polymerizable groups adjoin. Then, it is expected that M_n increases in the polymerization under a dc electric field. However, on application of the dc electric field the low molecular weight fractions in the GPC chart shown in Figure 5B increased and M_n of the resulting polymer decreased. The peak in the low molecular weight fractions may be due to a change in the microphase structure. Application of a dc electric field may decrease the diffusion of the system, and polymerization under a dc electric field might be strongly affected by a change in microphase structure.

III.3. Birefringence of Sample after Photoirradiation in the I Phase. Figure 8 shows the textures of the cell observed on a polarizing microscope at room temperature. These are the textures observed after irradiation in the I phase of FLC monomers for 60 s. After photoirradiation of **MS11**, birefringence was induced (Figure 8A). This result indicates that the phase changed from the I phase to the SmC_A* phase. In the case of monomer possessing a long spacer, the polymerizable group and the core are decoupled. Therefore, reorientation of the core occurs during polymerization. For **MS2**, no focal conic texture was confirmed (Figure 8B). The dark view has two possibilities: homeotropic SmA* phase or I phase. To determine the phase of sample after photoirradiation, the texture was examined with a conoscope by optical polarizing microscopy. If the sample exhibits the homeotropic SmA* phase, texture should be observed with the conoscope. However, no texture was detected with the conoscope. These results suggest that the sample after 60-s irradiation in the I phase showed an I phase. After 60-s photoirradiation of **MS2**, the phase should change from the I to the G phase via the SmA* phase during polymerization, since the conversion was higher than 70%. However, the phase remained in the I phase macroscopically. For a monomer with a short spacer, the polymerizable group and the core are coupled. Therefore, the highly disordered main chain of the polymer produced may have prevented the alignment of the core in such a way that

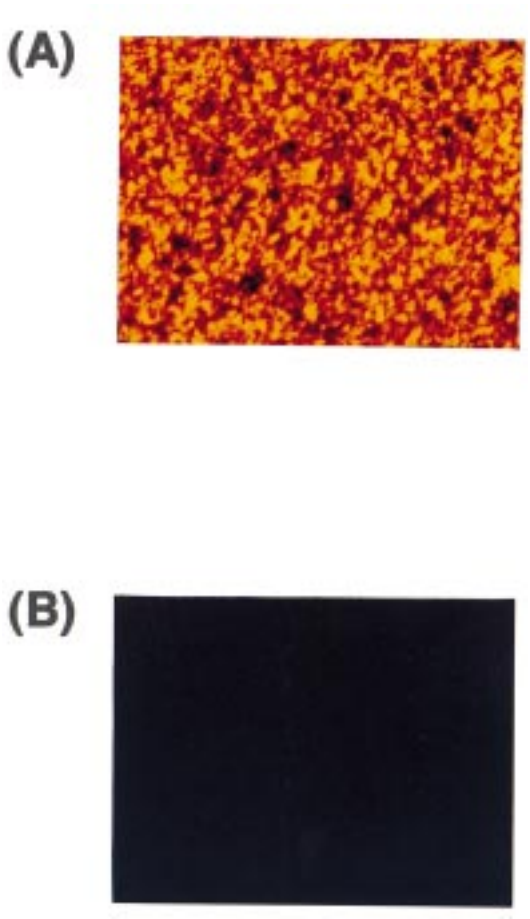

Figure 8. Polarized optical micrographs of the texture observed in the 2-μm-gap cell after 60-s photoirradiation (1 mW/cm^2) of FLC monomers without an electric field in the I phase: (A) texture of sample after photopolymerization of **MS11** at 85 °C; (B) texture of sample after photopolymerization of **MS2** at 80 °C.

the disordered I state of the core parts remained unchanged.

III.4. Alignment of Photopolymerized FLC. The molecular alignment of the FLCs was explored by optical polarizing microscopy after the photopolymerization of **MS11** was conducted in the 2-μm-gap cell at 60 °C in the SmC* phase. Before photoirradiation, the polarization flip was confirmed at first to occur by application of the alternating electric field ($\pm$3 V_{pp}/μm). The optical texture after photoirradiation was the same as that before photoirradiation, but the polymerized FLC showed no response to the electric field. This immobilization of molecular alignment could be attributed to the low mobility of mesogens of the polymerized FLC owing to volume shrinkage.[7] It is reasonable that the decrease of the mobility of mesogens by the polymerization results in no change in the molecular alignment, even in the presence of the external field.

Photopolymerization of monomer in the SmC* phase without an electric field produced the polydomain of the LC phase. The application of the external electric field to the sample resulted in appearance of the immobilized SmC* phase in which all mesogens of the polymerized FLC were aligned in one direction, leading to the formation of a monodomain of the LC phase. A similar result was obtained on photoirradiation of **MS2**. Such immobilization of the SmC* phase is quite favorable from the viewpoint of optical applications. For instance,

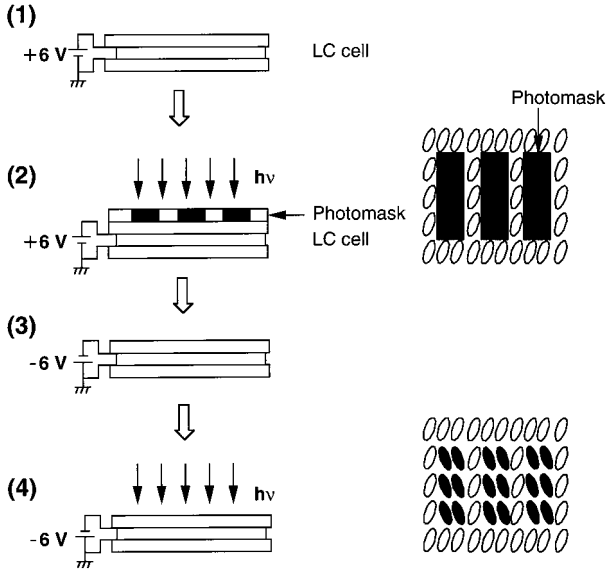

Figure 9. Diagram of image storage. (1) Dipoles of FLC molecules are aligned to produce polarization by external electric field. FLC molecules are also aligned into one direction. (2) With a photomask, the LC cell is irradiated, which leads to immobilization of mesogens by polymerization at the irradiated part. (3) The direction of the FLC molecules is changed by application of an electric field with reverse polarity. (4) The LC cell is again irradiated without the photomask to immobilize the other part of the cell.

image storage was expected by applying an electric field with reverse polarity, since the polarization flipped into the opposite direction only in the unpolymerized part. Image storage has been achieved by changing the direction of the applied magnetic field,[3j] and a network with a patternwise orientation has been prepared by locally applying electric fields.[13]

The diagram for the image storage is shown in Figure 9. An LC cell containing a monomer and a photoinitiator was covered with a photomask, LC molecules were aligned in the SmC* phase, and then photoirradiation was conducted with applying dc electric field for 60 s. The monomer was polymerized only in the irradiated part by this method. In this part, LC molecules showed no response to the electric field of 3 V_{pp}/μm. By application of an electric field with reverse polarity which was larger than the threshold value, the polarization flipped into the opposite direction in the unpolymerized part. After the photomask was removed, photoirradiation was conducted for 60 s again.

Image storage was achieved by photopolymerization of **MS11** while it was unsuccessful in **MS2**. As shown in Table 1, **MS2** exhibited a narrow monotropic SmC* phase upon cooling, and crystallization tended to occur quite rapidly upon removal of the photomask. However, the image could be stored by an alternative method. After the monomer in the irradiated part was polymerized (Figure 9(2)), the sample was heated to 80 °C (I phase in unreacted monomer) and was photoirradiated without the photomask. As described in the previous section, the I state of the core was maintained after photopolymerization of **MS2** monomer in the I phase. A bright view was observed for the former, whereas a dark view was seen for the latter. Figure 10 shows the texture of sample prepared by photoirradiation of **MS11** observed with a polarizing microscope in the cell with a 2-μm gap. We observed bright and dark views alternately every 45° by rotating the sample with respect to

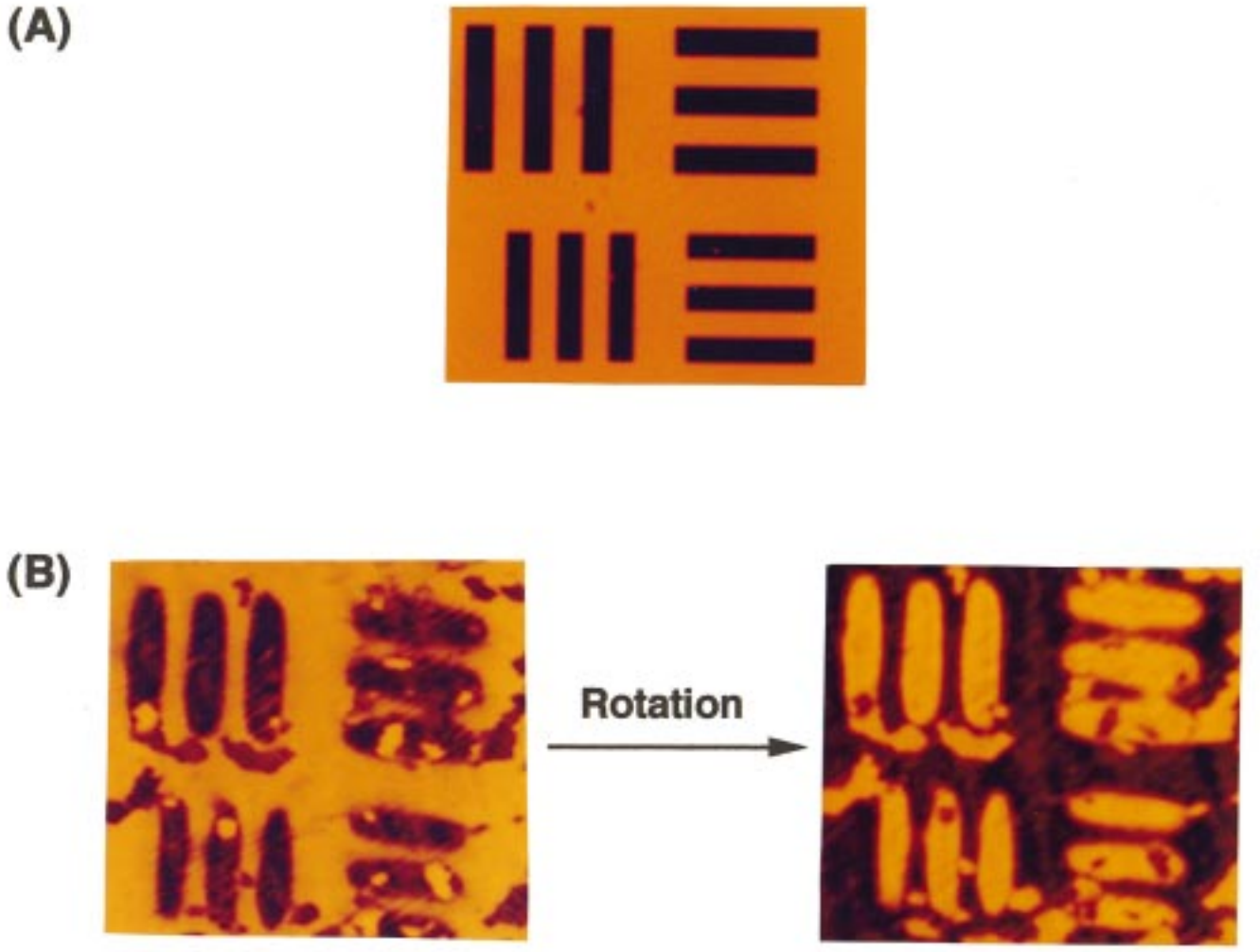

Figure 10. Image storage in polymerized **MS11**. Photoirradiation (1 mW/cm^2) was carried out at 60 °C. Key: (A) test pattern used as photomask; (B) stored image after 15 months.

the plane of polarization. Furthermore, the stored image obtained by photopolymerization in the ferroelectric phase has been stable for 2 years at room temperature. These results suggest that the procedure is applicable to optical recording.

IV. Conclusion

In situ photopolymerization behavior was evaluated using two FLC monomers with a polymerizable group attached to the rigid core through a long alkyl spacer and a short alkyl spacer. Polymerizability of **MS2** was considerably different from that of **MS11**. The change of macroscopic structure observed by applying an electric field was more effective in the polymerization of **MS2**. In addition, the methacrylate exhibited a polymerization behavior different from that of the corresponding acrylate. Furthermore, we conducted image storage by in situ photopolymerization of FLC monomer. The bistable FLC monomers enabled image storage by applying an electric field and the immobilization of the ferroelectric phase by in situ photopolymerization.

References and Notes

(1) (a) Clark, N. A.; Lagerwall, S. T. *Appl. Phys. Lett.* **1980**, *36*, 899. (b) Decobert, G.; Dubois, J. C.; Esselin, S.; Noël, C. *Liq. Cryst.* **1986**, *1*, 307. (c) Ouchi, Y.; Takezoe, H.; Fukuda, A.; Kondo, K.; Kitamura, T.; Yokokura, H.; Mukoh, A. *Jpn. J. Appl. Phys.* **1988**, *27*, L733. (d) Skarp, K.; Handschy, M. A. *Mol. Cryst. Liq. Cryst.* **1988**, *165*, 439. (e) Ikeda, T.; Sasaki, T.; Ichimura, K. *Nature* **1993**, *361*, 428. (f) Sasaki, T.; Ikeda, T.; Ichimura, K. *J. Am. Chem. Soc.* **1994**, *116*, 625. (g) Sasaki, T.; Ikeda, T. *J. Phys. Chem.* **1995**, *99*, 13002. (h) Sasaki, T.; Ikeda, T. *J. Phys. Chem.* **1995**, *99*, 13008. (i) Sasaki, T.; Ikeda, T. *J. Phys. Chem.* **1995**, *99*, 13013. (j) Trollsås, M.; Sahlén, F.; Gedde, U. W.; Hult, A.; Hermann, D.; Rudquist P.; Komitov, L.; Lagerwall, S. T.; Stebler, B.; Lindström, J.; Rydlund, O. *Macromolecules* **1996**, *29*, 2590.

(2) Fukuda, A.; Takezoe, H. *Structures and Properties of Ferroeletric Liquid Crystals*; Corona: Tokyo, 1990.

(3) (a) Broer, D. J.; Finkelmann, H.; Kondo, K. *Makromol. Chem.* **1988**, *189*, 185. (b) Hoyle, C. E.; Chawla, C. P.; Griffin, A. C. *Mol. Cryst. Liq. Cryst.* **1988**, *157*, 639. (c) Broer, D. J.; Mol, G. N. *Makromol. Chem.* **1989**, *190*, 19. (d) Broer, D. J.; Boven, J.; Mol, G. N. *Makromol. Chem.* **1989**, *190*, 2255. (e) Broer, D. J.; Hikmet, R. A. M.; Challa, G. *Makromol. Chem.* **1989**, *190*, 3201. (f) Hoyle, C. E.; Chawla, C. P.; Griffin, A. C. *Polymer* **1989**, *60*, 1909. (g) Broer, D. J.; Mol, G. N. *Makromol. Chem.* **1991**, *192*, 59. (h) Hoyle, C. E.; Kang, D.; Chawla, C. P.; Griffin, A. C. *Polym. Eng. Sci.* **1992**, *32*, 1490. (i) Hoyle, C. E.; Kang, D.; Jariwala, C.; Griffin, A. C. *Polymer* **1993**, *34*, 3070. (j) Hoyle, C. E.; Watanabe, T.; Whitehead, J. B. *Macromolecules* **1994**, *27*, 6581. (k) Broer, D. J.; Lub, J.; Mol, G. N. *Nature* **1995**, *378*, 467. (l) Kurihara, S.; Ohta, H.; Nonaka, T. *Polymer* **1995**, *36*, 849. (m) He, L.; Zhang, S.; Jin, S.; Qi, Z. *Polym. Int.* **1995**, *38*, 211.

(4) Paleo, M. *Chem. Soc. Rev.* **1985**, *14*, 45.

(5) (a) Paleos, C. M.; Labes, M. M. *Mol. Cryst. Liq. Cryst.* **1970**, *11*, 385. (b) Hoyle, C. E.; Chawla, C. P. *Macromolecules* **1995**,

26, 1946. (c) Guymon, C. A.; Hoggan, E. N.; Clark, N. A.; Rieker, T. P.; Walba, D. M.; Bowman, C. N. *Science* **1997**, *275*, 57.
(6) Finkelmann, H.; Ringsdorf, H.; Wendorff, J. H. *Makromol. Chem.* **1978**, *179*, 273.
(7) Ogiri, S.; Kanazawa, A.; Shiono, T.; Ikeda, T.; Nishiyama, I.; Goodby, J. W. *Macromolecules* **1998**, *31*, 1728.
(8) Nishiyama, I.; Goodby, J. W. *J. Mater. Chem.* **1993**, *3*, 169.
(9) Hoyle, C. E.; Watanabe, T. *Macromolecules* **1994**, *27*, 3790.
(10) Hoyle, C. E.; Kang, D. *Macromolecules* **1993**, *26*, 844.
(11) Brandrup, J.; Immergut, E. H.; McDowell, W. *Polymer Handbook*; Wiley: New York, 1975; pp II45−II104.
(12) He, L.; Zhang, S.; Jin, S.; Qi, Z. *Polym. Bull.* **1995**, *34*, 7.
(13) Hikmet, R. A. M.; Lub, J. *J. Appl. Phys.* **1995**, *77*, 6234.

MA9805607